Aust. J. Phys., 1978, **31**, 333–45

The Accuracy of Frequency Standards disseminated by HF Radio Paths through the Ionosphere

M. L. Heron[A,B] *and R. J. Rose*[A]

[A] Physics Department, James Cook University of North Queensland, Qld 4811.
[B] Present address: Ionospheric Physics Program, Space Environment Laboratory, Environmental Research Laboratories, National Oceanic and Atmospheric Administration, U.S. Department of Commerce, Boulder, Colorado 80302, U.S.A.

Abstract

The 12 MHz VNG standard frequency transmitted from Lyndhurst has been phase compared with a local standard at Townsville over a total of 54 days. The Doppler shift introduced by the one ionospheric reflection has a diurnal trend which is predictable from the ionosphere parameters $f_0 F_2$ and M3000F. The optimum time of day for frequency dissemination using VNG 12 is between 1100 and 1530 h. Faster fluctuations generally obscure the diurnal trend, however, and an accuracy of $\pm 0 \cdot 1$ Hz on the 12 MHz carrier is attainable only by averaging the incoming frequency over a 1 h period. Spectral analysis of the fluctuations in frequency show significant spectral amplitudes down to short periods of about 1 min where the time resolution of the measurements provides a cutoff. Fluctuations with periods around 20–100 min are explained in terms of travelling ionospheric disturbances, but the spectral amplitudes in the short-period region require special attention as the periods are shorter than the time constants of most phenomena in the F layer. It is suggested that rapid switching between dominating ray paths can account for the f^{-1} spectrum of 'noise' observed.

1. Introduction

Early observations of Doppler shifts on HF radio paths were directed towards diagnosing ionospheric dynamics. Sudden frequency deviations were reported for example by Fenwick and Villard (1960) and Davies *et al.* (1962) and were related to solar flares, sudden commencements of geomagnetic storms and other singular ionospheric events. These events can cause changes in the vertical distribution of ionospheric plasma over a time scale of several minutes. Such changes alter both the geometry of the ray path and the refractive index along the path and so will introduce frequency offsets at a receiver which are maintained for the duration of the ionospheric transience. Jacobs and Watanabe (1966) have derived a basic theory relating observed Doppler frequency offsets back to an electric field across the Earth's magnetic field. Such electric fields are present during magnetically disturbed periods. Lewis (1967) reported reasonably good agreement between pi 2 geomagnetic micropulsations and Doppler fluctuations, although there was not always a clear one to one relationship.

Georges (1968) used the spectral characteristics of fluctuations in ionospheric Doppler shift to study travelling disturbances in the upper atmosphere and categorized large-scale and medium-scale travelling ionospheric disturbances. Shorter period fluctuations of about 3 min periodicity were related to severe weather disturbances below the reflection point on all of about a dozen cases studied. Again, however, a good one to one relationship was not found as some severe storms did not yield the Doppler fluctuations.

There are obviously a multiplicity of causes for the degree of intensity in the various parts of the spectrum of Doppler fluctuations. The approach made in the present work is evaluative rather than diagnostic and the emphasis is in evaluating the predictability of the Doppler fluctuations on an HF signal. From the engineering point of view a knowledge of the mean Doppler offset is essential to enable frequency standard services such as WWV and VNG to be utilized to their best accuracy. Associated with this is the need to know what spectral degradation might be expected when ionospheric Doppler fluctuations are convoluted onto HF signals. Finally these data may be used to comment on previously suggested mechanisms for the observed fluctuations.

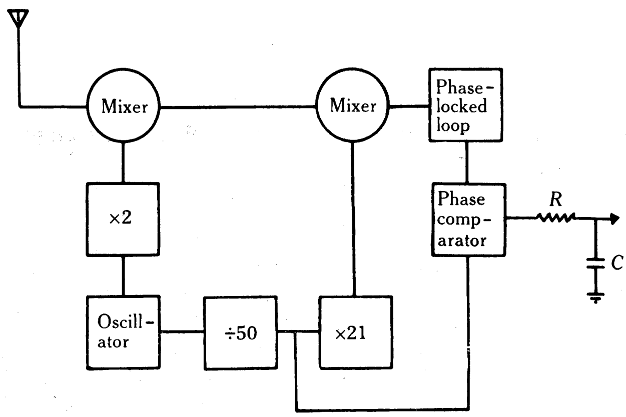

Fig. 1. Block diagram of the receiver showing the frequency offset arrangement and the phase comparator (oscillator frequency 4918032·377 Hz, *RC* time constant 0·1 s).

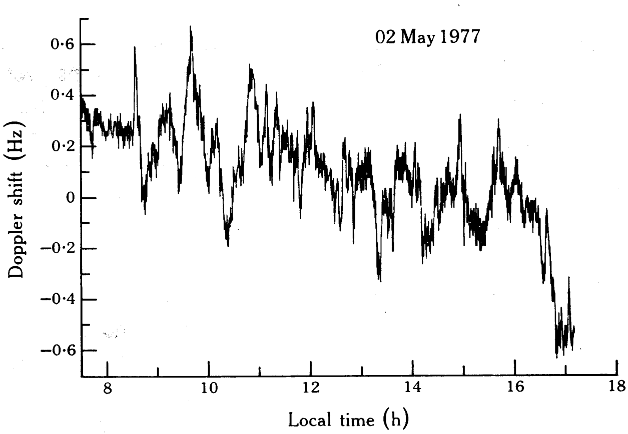

Fig. 2. Frequency fluctuations for a typical day on the 2000 km path.

2. Observations

A standard frequency (VNG 12) with 1 s time pips is transmitted from Lyndhurst, Victoria, on 12 MHz between 0745 and 1930 h AEST. This transmitter is maintained and operated by Telecom Australia as a national service and is based on a caesium standard. The signal is received at Townsville at a ground range of approximately

2000 km on a roughly north–south path. This combination of ground range and frequency effectively eliminates E layer propagation and, except for high sunspot epochs, the propagation is by one reflection from the ionospheric F layer.

In the present work, the VNG 12 signal received at Townsville during the daytime was phase compared with a local standard (1 part in 10^9 long term) using the system outlined in the block diagram of Fig. 1. The local standard at 5 MHz was deliberately offset for these observations so that positive and negative Doppler shifts could be resolved. The frequency of the phase-locked loop varied to follow the frequency of the highest amplitude component in the receiver band. The phase comparator had a time constant of 0·1 s which limited the rate of phase change observable. The phase comparator output was sampled and digitized 50 times per second and the phase variations were accumulated over intervals of 10 s. The net phase shift was recorded every 10 s for post analysis. The experiment was carried out over 54 days and a total of some $1 \cdot 14 \times 10^8$ observations were made.

Fig. 2 shows the variation in the Doppler offset throughout a typical day. The overall diurnal trend is almost masked by the rapid fluctuations, and this was so on all other days. Since the object of this work requires that these two components be separated, the diurnal trend is extracted by averaging data taken at the same time for similar days. Days are grouped seasonally, and Figs 4*a*, 4*b* and 4*c* in Section 3 below show data gathered on 21 summer days, 14 equinoctial days and 19 winter days respectively. This approach of averaging over similar days relies on the assumption that all fluctuations other than regular diurnal ones occur randomly. Diurnal patterns emerge quite clearly, and they are related to ionosonde observations in Section 3. The faster fluctuations are analysed by taking a Fourier transform for each day. The results are discussed in Section 4 and the spectral density of the Doppler fluctuations shown in Fig. 2 is plotted in Fig. 5. To obtain predictive statistics, the spectra for groups of days are superposed.

3. Diurnal Changes in Doppler Shift

There are several ways of predicting the Doppler frequency shift from vertical incidence ionograms. The most accurate of these is to use the transmission curve of virtual height versus frequency for 12 MHz propagation over the given ground range as an overlay on the ionogram (Davies 1965). The rate of change of virtual height can be used to calculate the Doppler frequency shift.

The method used here is an approximate one which depends on the accuracy of some assumed models but it has the advantage of using only the normally tabulated ionosonde data (Piggott and Rawer 1972), and evaluates changes in the estimated virtual height. In Fig. 3 the propagation path length P (km) is given by $R\sin\theta/\sin\phi$ and, if the virtual-height change in path length is

$$\Delta P = -\Delta\phi\, R\sin\theta\cos\phi/\sin^2\phi \quad \text{km}, \tag{1}$$

the frequency shift Δf is given by

$$\Delta f = -2000\,\Delta P/\Delta T\,\lambda \quad \text{Hz}, \tag{2}$$

where ΔT is the time interval in seconds and λ is the wavelength in metres. The factor of 2 allows for an identical down path.

To derive the virtual height from tabulated data, $h'F$ is used as an estimator of the height of the base of the F layer. A parabolic F layer is assumed to exist above that base and the tabulated $f_0 F_2$ value is taken to be the peak plasma frequency (critical frequency f_c). The virtual height h' for this model ionosphere is

$$h' = h'F + \tfrac{1}{2} Y_m (f_v/f_c) \ln\{(f_c + f_v)/(f_c - f_v)\}, \tag{3}$$

where $f_v = f \cos\phi$ is the equivalent vertical frequency and Y_m is the parabolic semi-thickness, which is twice the scale height of the atmosphere and is taken to be 100 km. Since equations (1) and (3) both involve the unknown ϕ they must be solved iteratively. This is a rapidly converging process.

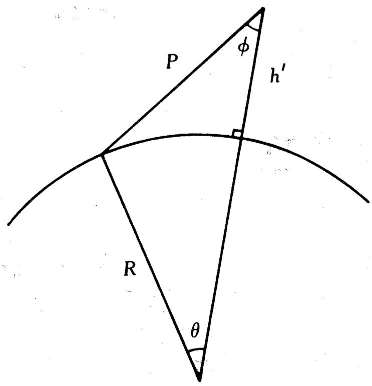

Fig. 3. Ray path geometry.

Equations (1) and (3) were solved at hourly intervals throughout the day using ionosonde data tabulated by the Australian Ionosphere Prediction Service for the Brisbane sounder. The differential time was then 1 h and the Doppler frequency offset Δf calculated from equation (2) was an average value over the hour.

The estimated hourly Δf values averaged over the days in the seasonal groupings are shown by the solid curves in Figs 4*a*, 4*b* and 4*c* and are compared with the averaged experimental offsets (points). To illustrate the basic ionospheric mechanism, the averaged hourly values of critical frequency are also plotted below in each figure along with the height of the peak of the F_2 layer calculated from tabulated M3000F values using Shimazaki's (1955) model.

The Doppler frequency is controlled by height and density changes in the F layer. When the critical frequency is increasing the virtual height is falling and if all else is constant the observed Doppler shift will be positive. On the other hand, if the layer is of constant density but rising then the Doppler shift will be negative. The observed offset frequency Δf depends on a dynamic balance between these two effects. This can be seen from Fig. 4*a* where Δf is kept positive between 730 and 1000 h by a steadily increasing plasma density. Between 1000 and 1200 h the rising layer appears to dominate and Δf goes negative. For a short period in the afternoon the layer is falling in height while the density is still increasing and, between 1400 and 1500 h, Δf is estimated to be just positive. After 1500 h the agreement between theory and observations is poor. On some days the critical frequency falls and the height of the layer rises to the point where the 12 MHz path closes. Such closure is preceded by

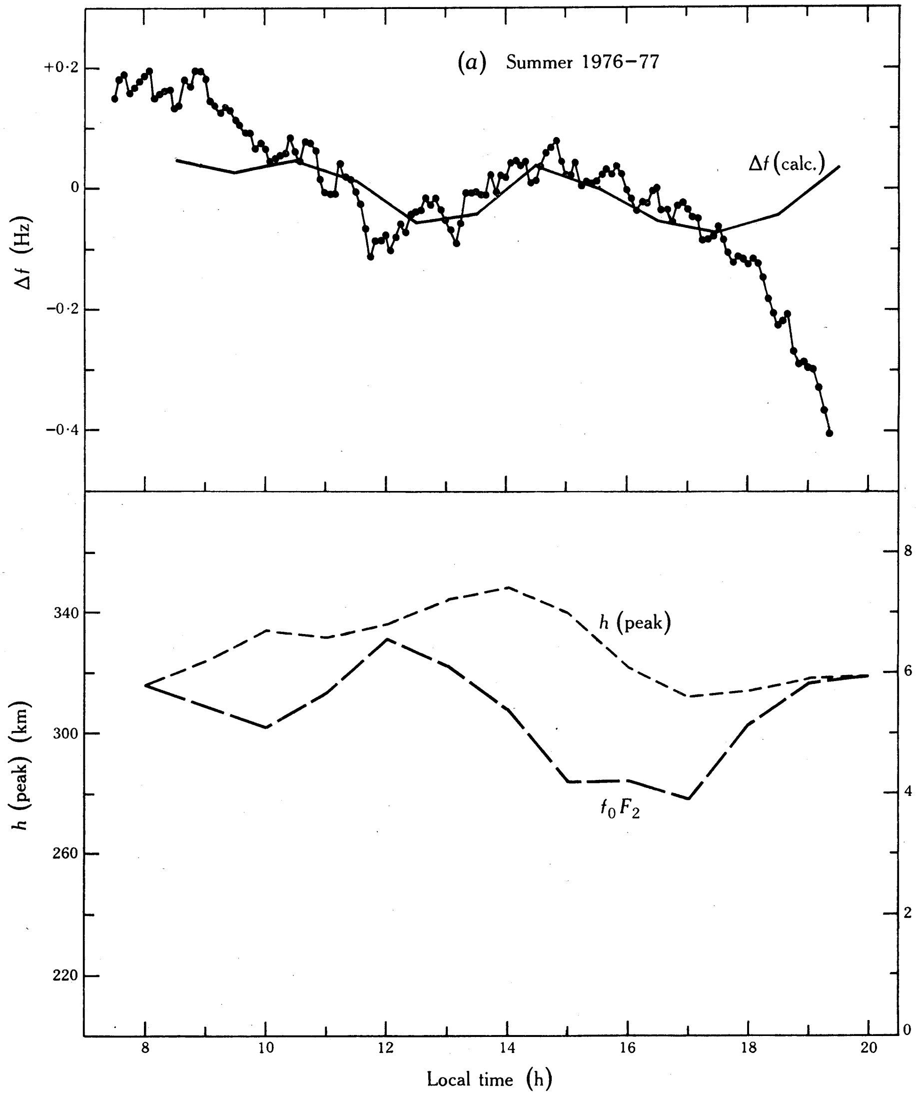

Figs 4*a*–4*c*. Comparisons of the experimental frequency fluctuations Δf (points) with the Doppler shifts calculated from ionogram data (solid curves), for values averaged over (*a*) 21 summer days (*b*) 14 autumn days and (*c*) 19 winter days. Shown below in each case (dashed curves) are averaged hourly values of the height h of the F layer peak and the critical frequency $f_0\,F_2$ derived from recorded data.

a large negative frequency shift. On other evenings the 12 MHz path is sustained by a slight increase in critical frequency, in which case the Doppler shift often goes positive. Similar results for groups of days in equinoctial and winter seasons are shown in Figs 4*b* and 4*c*, where the same trends can be seen.

The qualitative agreement obtained between estimated Doppler shifts and the experimental observations indicates that the general diurnal trends in ionospheric Doppler shifts are reconcilable with the tabulated ionogram data. From an operational

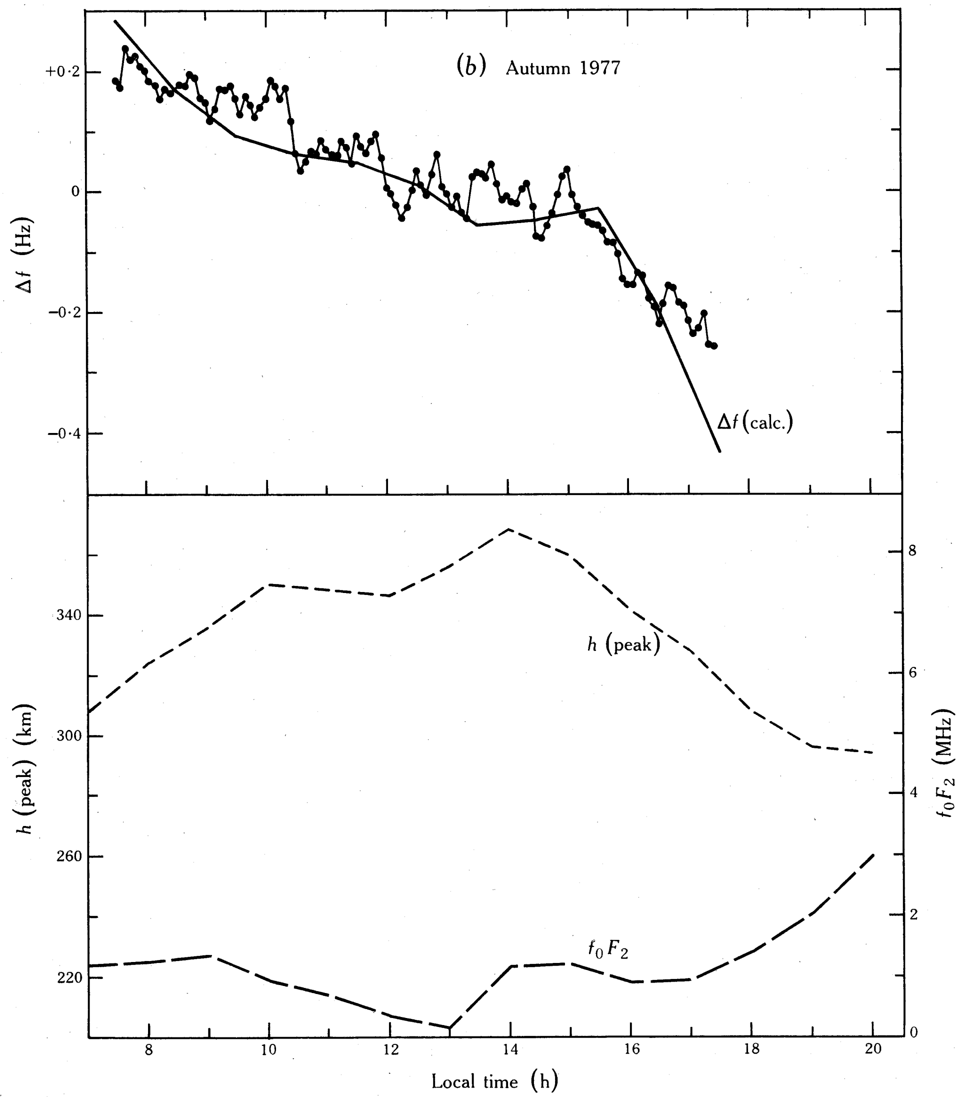

Fig. 4b

point of view the Ionosphere Prediction Service can be used to predict times of the day when minimum average ionospheric Doppler shifts occur. In a more subjective way, Ward (1972) chose 1400 h local time as the optimum, and Ward and Dexter (1976) operated the ocean backscatter HF radar near that time. The present results confirm that choice and show that the mean Doppler offset is most likely to be zero around 1300–1500 h local time and that the use of the HF standard frequency is optimal in this period. However, the departure from zero on any particular day is less predictable (see Fig. 2) and the fluctuations on a given day are normally greater than the mean offset frequency between 1000 and 1600 h.

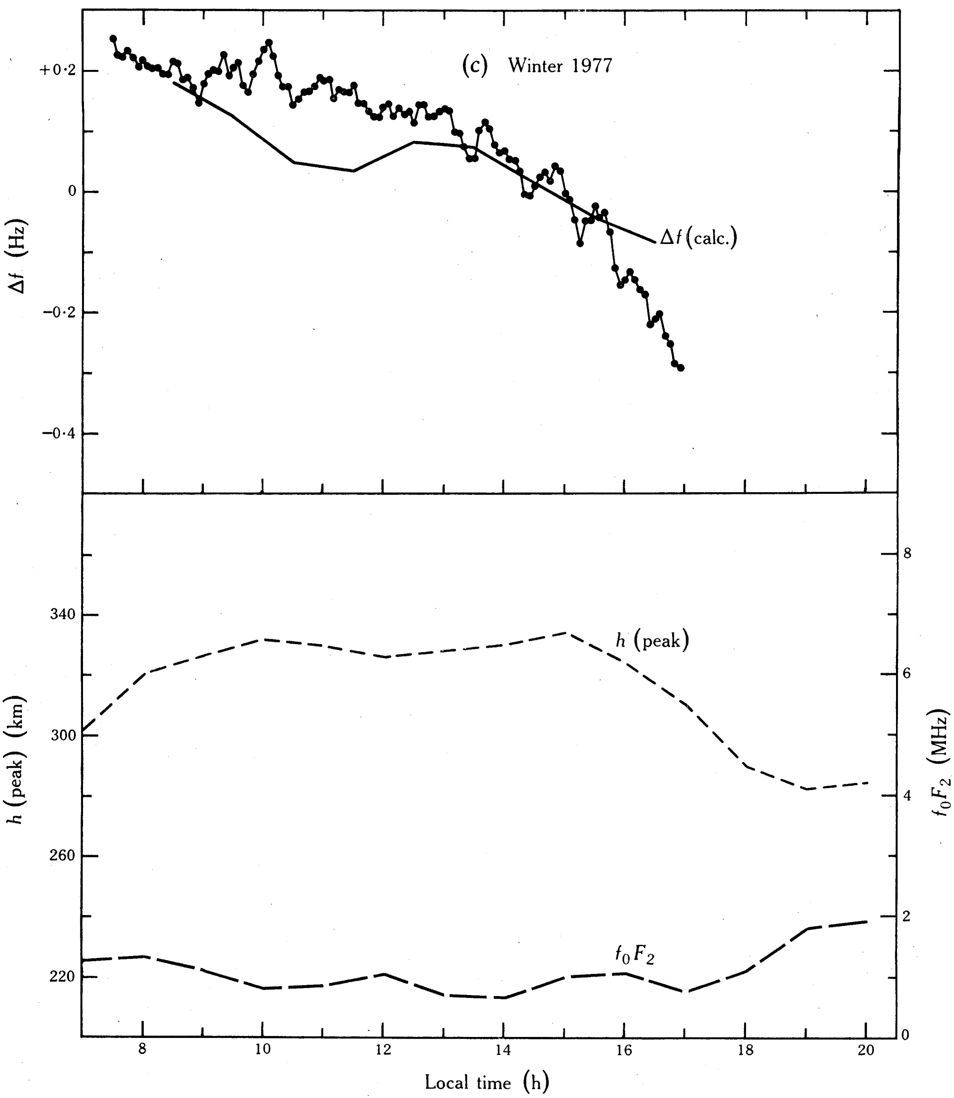

Fig. 4c

4. Fluctuations in Doppler Shift

(*a*) *Longer Period Fluctuations*

Because of the magnitude of the fast fluctuations it is they that impose the ultimate limitation on the accuracy of any oscillator set by comparison with an HF standard propagated via the ionosphere. In order to examine the fast changes, each full day of 10 s samples was transformed into a frequency spectrum. The spectrum of the time series shown in Fig. 2 for a typical day is plotted in Fig. 5. The mean of the time series was set to zero before the transformation and a Hanning window was used to cause roll-off for periods longer than the third harmonic. Fig. 5 is a spectrum of a time

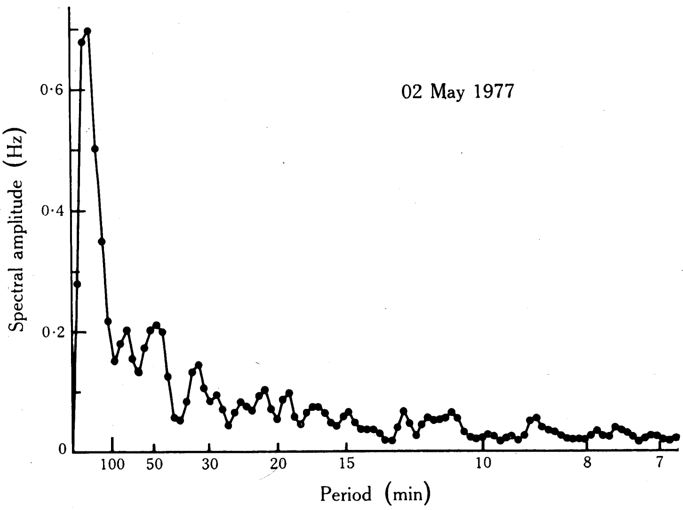

Fig. 5. Spectrum of Doppler frequency fluctuations for the typical day shown in Fig. 2. The main peak is false but the subsidiary peaks at 49 and 32 min relate to travelling ionospheric disturbances. The ordinate is the amplitude of each Fourier component over the complete data time interval.

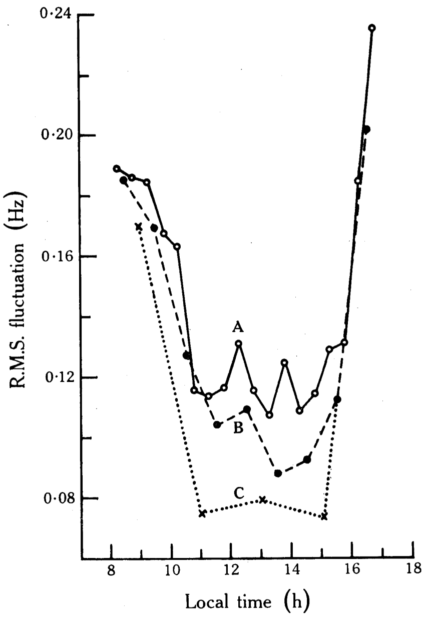

Fig. 6. Plots of r.m.s. frequency fluctuations for data averaged over:
A, $\frac{1}{2}$ h periods;
B, 1 h periods;
C, 2 h periods.
The average daily interval for minimal fluctuations is clearly defined to be 1100–1530 h.

varying frequency, sometimes referred to as a double spectrum. It shows a false peak in the third harmonic and subsidiary peaks at 49 and 32 min with measurable energy out to periods of a few minutes.

The long-period energy is associated with the diurnal effects as described in the previous section. The subsidiary peaks in the spectrum are produced by quasi-periodic fluctuations probably due to travelling ionospheric disturbances. In the example shown, the 49 min period is discernible in the morning (Fig. 2) and the shorter 32 min fluctuation in the afternoon. The time constant for morphological changes in the F layer plasma is greater than half an hour and the Brunt cutoff for propagating atmospheric gravity waves in the F region is 15–20 min (Titheridge 1972). The relationship between travelling ionospheric disturbances and fluctuations of periods greater than 15 min in the Doppler spectra has been discussed by Georges (1968) and others.

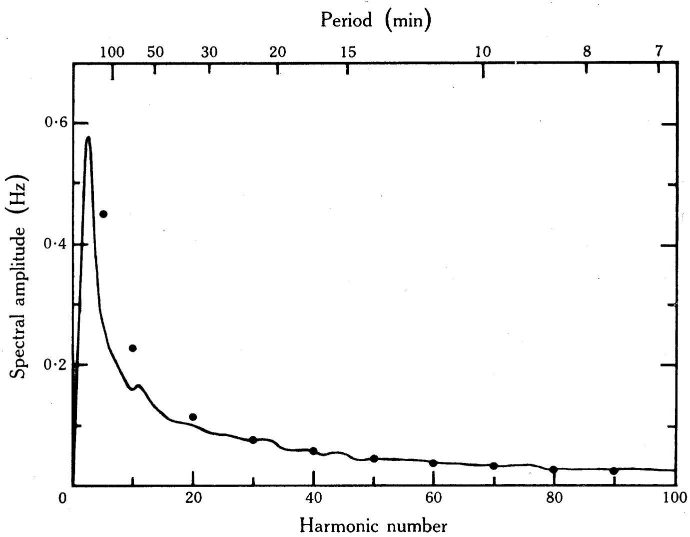

Fig. 7. Mean frequency fluctuation spectrum for all 54 days sampled. The points represent a curve with an f^{-1} form fitted to the spectral data for periods less than 30 min.

The present results suggest an optimum strategy for using the HF transmission as a reference. From the spectral point of view it might appear that an observation time longer than the dominant spectral component would be necessary. However, this is not feasible here since the fluctuations at about 4 h periodicity in the spectra originate from the diurnal trend. A better approach is to consider the phase relationships of the spectral components and to use the fact that the frequency versus time curves in Figs 4 exhibit a point of inflexion or even a return to positive frequencies around 1300 h. This inflexion regime was sought by calculating the r.m.s. frequency fluctuations. Values were calculated using means over $\frac{1}{2}$, 1 and 2 h intervals for all days, and the results are shown in Fig. 6. The r.m.s. values around midday were similar for the different seasons, and the only real seasonal difference was in summer when the r.m.s. values around 1600 and 1700 h were smaller. This relates to the evening increase in critical frequency on some summer days. Fig. 6 shows quite clearly that the best time to use HF paths for frequency standard dissemination is between 1100 and 1530 h. Averaging received frequencies over long periods within this interval reduces the expected r.m.s. deviation: average frequency offsets over 2 h periods had r.m.s. fluctuations of $0\cdot076$ Hz while those over $\frac{1}{2}$ h periods had r.m.s. fluctuations of about $0\cdot119$ Hz. For a white noise spectrum these values would be in the ratio 1 : 2, but the improvement obtained in these results by longer term averages is limited by diurnal trends, and a compromise must be made. If a 1 h working interval is used for HF oscillator calibrations at any time between 1100 and 1530 h then the expected error on the frequency setting will be about $\pm 0\cdot 1$ Hz.

(b) Fast Fluctuations

The spectrum shown in Fig. 5 from data for one day has energy at short periods down to 7 min, and further analysis showed a continuing trend as far as a 1 min period. Other daily spectra were similar, varying only in the random placement of small peaks, and the spectra for all days were superposed to obtain the mean spectrum shown in Fig. 7.

The presence of the residual energy at short periods is enigmatical as the time scale is far less than the time constants for chemical or kinetic changes in the ionosphere. Georges (1968) reported a similar almost constant spectral density over periods from 30 to 1000 s and attributed it to incoherent superposed gravity waves and weather. Sears (1970) confirmed the nearly white spectrum but an association with geomagnetic activity led him to argue, by way of the theory of Jacobs and Watanabe (1966), that the short-period fluctuations in the Doppler spectrum originate from changes in the geomagnetic field intensity. Magnetic field fluctuations and the associated electric fields cause plasma density fluctuations. While our results do not refute these explanations of the sustained energy at short periods, a simpler physical model can be suggested for the present data.

The general form of the mean spectrum in Fig. 7 is an f^{-1} decrease, shown by the plotted points, and this is a reasonably good fit down to a 1 min period. The best overall value of the exponent is about $-0 \cdot 86$. These measurements were made with the aid of a single phase-locked oscillator which always followed the phase of the strongest signal in the band.

If the dominant ray path switches from one part of an assembly of ionospheric irregularities to another then sudden steps in frequency occur. Each of the possible reflection points in such an assembly has its own movement. Thus in the interval of a few minutes the dominant path can switch several times between paths whose reflection regions are undergoing different vertical displacements, each imposing its own Doppler shift on the wave. It is reasonable therefore to expect noise in the spectrum originating from a series of step functions with varying sign and separation in the time data. An analysis of this situation based on a series of randomly occurring rectangular pulses with fluctuating amplitude and duration is given in the Appendix. If we estimate that the noise-free amplitude spectrum $F(\omega)$ varies as ω^{-1} then

$$F(\omega) \propto \omega^{-1},$$

and for small frequencies ($\omega \ll 2/T$ where T is the median random pulse duration) the total amplitude spectrum is obtained from equation (A2) in the Appendix:

$$Y(\omega) \approx \omega^{-1}(a+b\omega)^{\frac{1}{2}},$$

where a and b are constants. For frequencies such that $\omega \approx 2/T$ we have

$$Y(\omega) \approx c\omega^{-1},$$

where the coefficient c is subject to some random fluctuations arising from the summations in equation (A1). For high frequencies ($\omega \gg 2/T$),

$$Y(\omega) = d\omega^{-1},$$

where d is constant (equation A3).

If the noise-free amplitude spectrum follows a power law of index slightly different from -1, as might be suggested by the best fit value of $-0\cdot86$, then the noise spectrum will also differ. Irrespective of such deviations the inherent step noise mechanism gives a spectral tail of the general form observed. There may be other forms of impulsive noise in the data which contribute in a similar way to the short-period tail of the spectrum.

5. Conclusions

We have seen that HF radio waves transmitted by reflection off the ionosphere are subject to Doppler shifts imposed on the signal by the dynamic irregular structure of the ionosphere and also by the regular diurnal plasma density changes. Analysis of the present data has shown that the mean diurnal trend is generally predictable from the recorded ionosphere parameters of critical frequency and peak height. There is a near zero mean frequency offset at about 1300 h. However, fluctuations on any day generally obscure the diurnal trend. The spectral energy at periods above about 2 h is a combination of the regular diurnal trend and less predictable morphological changes in height and density of the reflecting layer. Secondary spectral peaks at periods down to about half an hour are a result of quasi-periodic travelling ionospheric disturbances.

The optimum time of day to use HF signals as frequency standards is between 1100 and 1530 h. If a 1 h observation interval is used during this optimum period then an absolute accuracy of $\pm0\cdot1$ Hz can be obtained on the 12 MHz carrier.

The spectrum of Doppler fluctuations has been seen to have significant amplitudes down to periods of 1 min, a time scale that is shorter than the time constants for gas–plasma processes in the ionosphere. While these fast fluctuations may be sometimes associated with lower altitude meteorological storms or with geomagnetic micropulsations, our data are subject to a noise mechanism which adequately explains the high frequency energy. Small movements of isoionic contours near the point of reflection can quickly change the path of the dominant ray. At the time of ray-path switching, the Doppler shift will also change abruptly from the time derivative of one ray path to that of the next. Such an assembly of random step functions in time is shown to have an approximately f^{-1} amplitude spectrum at the high frequency end. Since the energy in this short-period end of the spectrum is present on all days in the present data it would appear to originate from a noise source rather than meteorological or geomagnetic disturbances.

Acknowledgments

This work has been carried out with financial assistance from the Radio Research Board (Australia) and continues a program begun in 1971 at James Cook University with financial assistance from Telecom Australia. We thank Professor J. F. Ward for his interest in the project. Preparation of the final manuscript was undertaken at the Space Environment Laboratory, NOAA, whilst M.L.H. was a research associate of the University of Colorado.

References

Davies, K. (1965). 'Ionospheric Radio Propagation', NBS Monograph 80, p. 166 (U.S. Govt: Washington, D.C.).

Davies, K., Watts, J. M., and Zacharisen, D. M. (1962). *J. Geophys. Res.* **67**, 601.

Fenwick, R. C., and Villard, O. G. (1960). *J. Geophys. Res.* **65**, 3249.
Georges, T. M. (1968). *J. Atmos. Terr. Phys.* **30**, 735.
Jacobs, J. A., and Watanabe, T. (1966). *Radio Sci.* **1**, 257.
Lewis, T. J. (1967). *Can. J. Phys.* **45**, 1549.
Piggott, W. R., and Rawer, K. (1972). 'URSI Handbook of Ionogram Interpretation and Reduction' (U.S. Govt: Washington, D.C.).
Sears, R. D. (1970). *Radio Sci.* **5**, 1147.
Shimazaki, T. (1955). *J. Radio Res. Lab. Jpn* **2**, 85.
Titheridge, J. E. (1972). *Planet. Space Sci.* **19**, 1593.
Ward, J. F. (1972). Phys. Dept, James Cook Univ., Natural Philos. Rep. No. 23.
Ward, J. F., and Dexter, P. E. (1976). *Aust. J. Phys.* **29**, 183.

Appendix. Spectral Noise of Random Steps

The nature of the measurements described in the text requires the evaluation of abrupt random steps in the time domain data. Let the time series be represented by a smooth function $f(t)$ added to a noise function $n(t)$ which is made up of randomly occurring rectangular pulses whose duration T_j and amplitude A_j are distributed according to some probability density functions. The precise forms of the probability density functions do not need to be specified but a skew distribution similar to that of Poisson is a likely form. Interpretation of the following equations is most easily made if the distribution of the T_j values has a peak with a definable width ΔT.

The time domain function is

$$y(t) = f(t) + n(t)$$

and the Fourier transform $Y(\omega)$ is given by

$$Y(\omega) = \int_{-\infty}^{\infty} \{f(t) + n(t)\}\exp(-\mathrm{i}\omega t)\,\mathrm{d}t = F(\omega) + \sum_j (A_j/\omega)\sin(\tfrac{1}{2}\omega T_j),$$

where $F(\omega)$ is the transform of $f(t)$. The power spectrum is

$$P(\omega) = \{Y(\omega)\}^2 = \{F(\omega)\}^2 + 2F(\omega)\sum_j (A_j/\omega)\sin(\tfrac{1}{2}\omega T_j) + \left(\sum_j (A_j/\omega)\sin(\tfrac{1}{2}\omega T_j)\right)^2. \tag{A1}$$

For $\omega \ll 2/T_j$ we have

$$P(\omega) \approx \{F(\omega)\}^2 + 2F(\omega)\sum_j \tfrac{1}{2}A_j T_j + \left(\sum_j \tfrac{1}{2}A_j T_j\right)^2,$$

and assuming $A_j T_j \ll F(\omega)$, i.e. that the noise amplitude is small compared with the real fluctuations, this becomes

$$P(\omega) \approx \{F(\omega)\}^2 + 2F(\omega)\sum_j \tfrac{1}{2}A_j T_j. \tag{A2}$$

Obversely if we have $\omega \gg 2/T_j$ such that the spread of $\tfrac{1}{2}\omega\,\Delta T$ is greater than π radians then $\sin(\frac{1}{2}\omega T_j)$ becomes distributed through ± 1 and odd-powered summations probably self-cancel, so that

$$P(\omega) \approx \{F(\omega)\}^2 + \sum_j (A_j/\omega)^2 \tfrac{1}{2}\pi . \tag{A3}$$

In summary, the low frequency additive noise power is generally proportional to the spectral amplitude $F(\omega)$ (equation A2); at mid frequencies, noise power proportional to ω^{-2} is also added and fluctuations appear in the summation coefficients (equation A1); at high frequencies, the added noise power is a continuum proportional to ω^{-2}.

Manuscript received 30 November 1977